JB Journals.ASM.org

Ght Protein of *Neisseria meningitidis* Is Involved in the Regulation of Lipopolysaccharide Biosynthesis

Florian Putker, Andreas Grutsch, Jan Tommassen, Martine P. Bos*

Department of Molecular Microbiology and Institute of Biomembranes, Utrecht University, Utrecht, Netherlands

Lipopolysaccharide (LPS) is a major component of the outer membrane of Gram-negative bacteria and is responsible for the barrier function of this membrane. A *ght* mutant of *Neisseria meningitidis* that showed increased sensitivity to hydrophobic toxic compounds, suggesting a breach in this permeability barrier, was previously described. Here, we assessed whether this phenotype was possibly caused by a defect in LPS transport or synthesis. The total amount of LPS appeared to be drastically reduced in a *ght* mutant, but the residual LPS was still detected at the cell surface, suggesting that LPS transport was not impaired. The *ght* mutant was rapidly overgrown by pseudorevertants that produced normal levels of LPS. Genetic analysis of these pseudorevertants revealed that the *lpxC* gene, which encodes a key enzyme in LPS synthesis, was fused to the promoter of the upstream-located *pilE* gene, resulting in severe *lpxC* overexpression. Analysis of *phoA* and *lacZ* gene fusions indicated that Ght is an inner membrane protein with an N-terminal membrane anchor and its bulk located in the cytoplasm, where it could potentially interact with LpxC. Cell fractionation experiments indeed indicated that Ght tethers LpxC to the membrane. We suggest that Ght regulates LPS biosynthesis by affecting the activity of LpxC. Possibly, this mechanism acts in the previously observed feedback inhibition of LPS synthesis that occurs when LPS transport is hampered.

The cell envelope of Gram-negative bacteria consists of two membranes separated by the periplasm containing the peptidoglycan layer. The inner membrane (IM) is a phospholipid bilayer, while the outer membrane (OM) is an asymmetrical bilayer containing phospholipids and lipopolysaccharides (LPSs) in the inner and outer leaflets, respectively. LPS consists of at least two distinct parts, a hydrophobic membrane anchor called lipid A and an oligosaccharide core moiety. The core is in some cases extended with a polysaccharide consisting of repeating sugar groups, called the O antigen. After the lipid A-plus-core moiety is synthesized on the cytoplasmic side of the IM, it is flipped by the ABC transporter MsbA to the periplasmic side (1, 2), where the O antigen, if present, is attached to form mature LPS. While all enzymes involved in LPS synthesis have been identified in *Escherichia coli* (3), the exact mechanism of LPS transport to its final destination, the outer leaflet of the OM, remains to be elucidated. Until now, seven proteins were found to be involved in the transport of LPS from the periplasmic leaflet of the IM to the outer leaflet of the OM (4–8). These proteins, called LptA to LptG, presumably form a *trans*-envelope complex, as evidenced by their cofractionation (9). LptB, -F, and G form an ABC transporter in the IM that provides the energy for transport (10, 11). LptC and LptA supposedly form a bridge connecting the IM and OM components. In the OM, the integral membrane protein LptD forms a complex with the lipoprotein LptE (8, 12). LptE assists in the biogenesis of LptD (13, 14) and additionally may function to plug the pore in the β-barrel of LptD (15, 16). At least for *Neisseria meningitidis*, a direct role of LptE in LPS transport was excluded (17). Strong evidence for the transport of LPS via a *trans*-envelope bridge was provided by the finding that LPS transport continues in spheroplasts, which lack soluble periplasmic proteins (18).

We are studying LPS biogenesis in *N. meningitidis*. Whereas LPS is essential in many Gram-negative bacteria, including *E. coli*, this is not the case for *N. meningitidis* (19). Also, the genes encoding LPS transport functions can be knocked out in *N. meningitidis* (4, 17, 20), making it a very useful model organism to study LPS biogenesis. Interestingly, we detected strongly reduced LPS levels in LPS transport mutants of *N. meningitidis* (4, 17, 20), suggesting that LPS synthesis is inhibited when transport fails. The mechanism of this feedback inhibition is not known.

Here, we studied the potential involvement of a new protein in LPS biogenesis. Rasmussen et al. identified a gene, named *ght* (corresponding to locus tags NMB0339 and NMH_1913 in the genome sequences of strains MC58 [21] and H44/76 [22], respectively), in *N. meningitidis* whose absence resulted in an increased sensitivity to hydrophobic agents such as heme (23). Such a phenotype is diagnostic for a compromised OM. Therefore, we hypothesized that *ght* could play a role in LPS biogenesis.

MATERIALS AND METHODS

Bacterial strains and growth conditions. Strains used in this study are listed in Table 1. *N. meningitidis* strains were grown on GC plates (Oxoid) supplemented with Vitox (Oxoid) at 37°C in candle jars. The medium was supplemented with antibiotics when appropriate (kanamycin at 100 μg/ml and chloramphenicol at 5 μg/ml). Cultures were grown in 25-ml plastic flasks (Corning) in tryptic soy broth (TSB) (Scharlau) at 37°C with shaking (110 rpm). To obtain fully sialylated LPS, 80 μM cytidine 5′-monophospho-*N*-acetyl neuraminic acid (CMP-NANA) (Sigma) was added for 2 h to the medium of bacteria growing in mid-log phase. Expression of genes under *lac* promoter control was induced by using 1 mM isopropyl-β-D-thiogalactopyranoside (IPTG). *E. coli* strain DH5α was grown in LB broth or on LB plates supplemented with the appropriate antibiotics (chloramphenicol at 25 μg/ml and kanamycin at 50 μg/ml).

Received 9 August 2013 Accepted 27 November 2013

Published ahead of print 2 December 2013

Address correspondence to Jan Tommassen, j.p.m.tommassen@uu.nl.

* Present address: Martine P. Bos, Microbiome/VU Medical Center, Amsterdam, Netherlands.

doi:10.1128/JB.00943-13

TABLE 1 Strains used in this study

Strain	Characteristic(s)	Reference
E. coli DH5α	F$^-$ Δ(*lacZYA-algF*)*U169 thi-1 hsdR17 gyrA96 recA1 endA1 supE44 relA1 phoA* ϕ80d*lacZ*ΔM15	47
N. meningitidis		
HB-1	H44/76 with the entire capsule locus, including the *galE* gene, replaced by an *ermC* cassette	48
HB-1Δ*ght*	HB-1 with *ght* replaced by a Kan^r cassette	This study
HB-1Δ*lptH*	HB-1 with *lptH* replaced by a Kan^r cassette	17
HB-1Δ*lptD*	HB-1 with *lptD* largely replaced by a Kan^r cassette (formerly designated HB-1Δ*imp*)	4
HB-1Δ*lpxA*	HB-1 with a Kan^r cassette inserted at position 293 of *lpxA*	19
HB-1Δ*ght*(pGht)	HB-1Δ*ght* containing pEN11-Ght	This study
H44/76 L3	Wild-type serogroup B strain H44/76 expressing L3-immunotype LPS	4
H44/76 L3Δ*ght*	H44/76 L3 with *ght* replaced by a Kan^r cassette	This study
H44/76 L3Δ*lptD*	H44/76 L3 with *lptD* largely replaced by a Kan^r cassette	4
H44/76 L8(pPagL)	Wild-type serogroup B strain H44/76 expressing L8-immunotype LPS containing pEN11-PagL	4
H44/76 L8Δ*ght*(pPagL)	H44/76 L8(pPagL) with the chromosomal copy of *ght* replaced by a Kan^r cassette	This study
H44/76 L8Δ*lptD*(pPagL)	H44/76 L8(pPagL) with the chromosomal copy of *lptD* replaced by a Kan^r cassette	This study
HB-1Δ*ght*(pHis-Ght)	HB-1 containing pEN11-His-Ght with the chromosomal copy of *ght* replaced by a Kan^r cassette	This study
HB-1Δ*ght-rev1*	Pseudorevertant of HB-1Δ*ght* producing normal levels of LPS	This study
HB-1Δ*ght-rev2*	Pseudorevertant of HB-1Δ*ght* producing normal levels of LPS	This study
HB-1Δ*ght*(pLpxC)	HB-1 containing pEN21-LpxC with the chromosomal copy of *ght* replaced by a Kan^r cassette	This study
HB-1Δ*ght*(pLpxA)	HB-1 containing pEN11-LpxA with the chromosomal copy of *ght* replaced by a Kan^r cassette	This study
HB-1Δ*lptD*(pLpxC)	HB-1 containing pEN21-LpxC with the chromosomal copy of *lptD* largely replaced by a Kan^r cassette	This study
HB-1(pStrep-LpxC)	HB-1 containing pEN21-Strep-LpxC	This study
HB-1Δ*ght*(pStrep-LpxC)	HB-1 containing pEN21-Strep-LpxC with the chromosomal copy of *ght* replaced by a Kan^r cassette	This study
HB-1Δ*asmA*	HB-1 with *asmA* replaced by a Kan^r cassette	This study

Expression of genes under *lac* or *ara* promoter control was induced by using 1 mM IPTG or 0.66 mM L-arabinose (Sigma), respectively.

Construction of plasmids. The genome sequences of *N. meningitidis* strain MC58 (21) and *E. coli* K-12 strain MG1655 (24) were used to design primers. Genomic DNA was isolated as described previously (25). Plasmids and primers are listed in Tables 2 and 3, respectively. All new constructs described below were verified by sequencing.

A deletion construct of *ght* was obtained by amplifying DNA frag-

TABLE 2 Plasmids used in this study

Plasmid	Characteristic(s)	Source or reference
pCRII-TOPO	TA cloning vector	Invitrogen
pCRII-Δ*ght*	pCRII-TOPO containing a *ght* inactivation construct	This study
pCRII-strep-*lpxC*	pCRII-TOPO containing *lpxC* with a 5′ sequence for Strep-tag II	This study
pMB25	pCRII-TOPO carrying an *lptD* inactivation construct	4
pEN11-Imp	*Neisseria* replicative plasmid containing *imp* (renamed *lptD*) behind a dual *lacUV5-tac* promoter; this plasmid carries Cat^r and Erm^r cassettes	4
pEN11-Ght	pEN11-Imp derivative with *imp* replaced by *ght*	This study
pEN11-His-Ght	pEN11-Imp derivative with *imp* replaced by 6×His-tagged Ght	This study
pEN11-PagL	pEN11-Imp derivative with *imp* replaced by *pagL* from *B. bronchiseptica*	4
pEN11-LpxC	pEN11-Imp derivative with *imp* replaced by *lpxC*	This study
pEN11-LpxA	pEN11-Imp derivative with *imp* replaced by *lpxA*	This study
pEN21	pEN11 derivative with the *lacUV5-tac* promoter replaced by a *tac* promoter	This study
pEN21-LpxC	pEN21 containing *lpxC*	This study
pEN25	pRIT16860 with the dual *lacUV5-tac* promoter replaced by a *tac* promoter	This study
pEN21-Strep-LpxC	pEN21 encoding LpxC with an N-terminal Strep-tag II	This study
pBAD*lacZ*	pBAD*phoA* in which *phoA* is replaced by a *lacZ*α fragment	This study
pBAD*phoA*	pBAD22 derivative encoding alkaline phosphatase without signal sequence	49
pBAD*yciM-lacZ*	pBAD*lacZ* in which *yciM* is fused to the 5′ end of *lacZ*α	This study
pBAD*yciM-phoA*	pBAD*phoA* in which *yciM* is fused to the 5′ end of *phoA*	This study
pJGA07	pMPM-K4Ω containing an *xcpT-phoA* fusion under *araBAD* promoter control	37
pMMB67EH	Broad-host-range vector	50
pUC19	Cloning vector encoding the LacZα fragment	51
pUC21	Cloning vector	51
pUC21-*kan*	pUC21 carrying a Kan^r cassette	This study
pUC21-Δ*asmA*	pUC21 containing an *asmA* inactivation construct	This study
pRIT16860	pEN11 derivative with the Cat^r and Erm^r cassettes replaced by a Kan^r cassette	GlaxoSmithKline

TABLE 3 Primers used in this study

Primer	Sequence (5′–3′)[a]	Restriction site
NMB0338-for	CTGCCGCATCCTATCCG	
NMB0338-rev	ATGTCGACATCGGCTTTCTTAAGGCTG	AccI
NMB0340-for	ATGTCGACAAATGGCAGACGTTTAC	AccI
NMB0340-rev	ATTGGCGGCGGCGGTATCAG	
NMB0339-for	ATCATATGGACAACGAATTGTGGATTATC	NdeI
NMB0339-rev	ATGACGTCGTGGTTAAACTTCGATTTTATTC	AatII
yciM-for-kpnI	AGTCGGTACCGCTGGAGTTGTTGTTTC	KpnI
yciM-rev-kpnI	CTAGGGTACCAGGCCATCAAGACCGCG	KpnI
lacZ-for	GCTAGCAGGAGGAATTCACCATGACCATGGACGTCCCAAGCTATTTAGGTGACAC	NheI
lacZ-rev	GTCGACCTAGGCGCCCGATGGCCCACTACGTGAACC	SalI
yciM-lacZ-for	GACGTCATGCTGGAGTTGTTGTTTCTG	AatII
yciM-lacZ-rev	GACGTCCAGGCCATCAAGACCGC	AatII
0339-for-his	ATCATATGCACCATCATCATCATCATAGCATCCCTTCGGGATTTTAT	NdeI
lpxC-for-ndeI	ATCGCATATGCTGCAAAGAACTTTG	NdeI
lpxC-rev-aatII	ATCGGACGTCTTATCCACAAGTTCTG	AatII
lpxA-pEN-for	ATCATATGACCCTCATCCACCCG	NdeI
lpxA-pEN-rev	ATGACGTCTCAGCGGATGATGCCGCGCGC	AatII
tac-for	GCGCTAAGATCTCTACTGAGCGCTGCCGCACAGCTCCATAG	BglII
tac-rev	CCGGGTACCGAGCTCGAATTCTGTTTCCTG	EcoRI
strep-lpxC-for	CATATGTGGTCTCATCCGCAATTCGAGAAGATGCTGCAAAGAACTTTGGCGAAATCC	NdeI
NMB1693-upF	GCGCCGAGATCTATGCGGTCTGTTCCGCC	BglII
NMB1693-upR	CCATGGCCGATAATAAATCCATAGCC	NcoI
NMB1693-dnF	CATATGACCCTGCTGGAACAATGGCAGTG	NdeI
NMB1693-dnR	GATATCGTTGAACGAAGTGTTCGTACCG	EcoRV
M13F	GTAAAACGACGGCCAGT	
M13R	GCGGATAACAATTTCACACAGG	
asmAF	CATATGGATTTATTATCGGTTTTCCACAAATAC	
asmAR	GACGTCTTACGGTTCTTTAGGTTTGAG	
pilE-for	ATGAACACCCTTCAAAAAGGTTTTAC	
lpxC-dn-rev	GCGCGGAGATCTTTATCCACAAGTTCTGATGTTCAGC	
ermC-qPCR-for	GGTCTATTTCAATGGCAGTTACG	
ermC-qPCR-rev	TATCTTTGAAATCGGCTCAGG	
lpxC-Fq	TGAAAACAGCGGGATTTCCT	
lpxC-Rq	AAGGCGGGTATCGTTGATCA	
omp85q-F	GAGATTCAGAACCGCATGGG	
omp85q-R	CAGGACGAAATCGACGGTTTT	
rpmEq-F	CTCTTGCGGCAACAAATTC	
rpmEq-R	TTTGGGTGCCGGTATAGAAC	

[a] Restriction sites are underlined.

ments flanking *ght* by PCR using primer pairs NMB0338-for/NMB0338-rev and NMB0340-for/NMB0340-rev and genomic DNA from strain HB-1. The fragments were cloned separately into pCRII-TOPO and then joined together in one plasmid using the AccI sites that were introduced via the primers and the XbaI site in the vector. The kanamycin resistance (Kan^r) cassette including the neisserial DNA uptake sequence from pMB25 was inserted using AccI restriction and ligation, yielding pCRII-Δ*ght*.

To create a plasmid carrying a wild-type copy of *ght*, the gene was amplified by using NMB0339-for and NMB0339-rev, cloned into pCRII-TOPO, and subcloned into pEN11 using NdeI and AatII restriction.

For the construction of the *yciM-phoA* fusion, *yciM* was amplified from genomic DNA of strain DH5α with primers yciM-for-kpnI and yciM-rev-kpnI and introduced into pCRII-TOPO. From there, *yciM* was excised by using KpnI and ligated into KpnI-restricted and shrimp alkaline phosphatase-treated pBAD*phoA*, yielding pBAD*yciM-phoA*. For the *yciM-lacZ* fusion, a *lacZ*α fragment was amplified from pCRII-TOPO by using primers lacZ-for and lacZ-rev, which was used to replace the *phoA* fragment in pBAD*phoA* using NheI and SalI restriction, resulting in pBAD*lacZ*. *yciM* was amplified from genomic DNA of strain DH5α with primers yciM-lacZ-for and yciM-lacZ-rev, inserted into pCRII-TOPO, and then subcloned into pBAD*lacZ* using AatII restriction and ligation, yielding pBAD*yciM-lacZ*.

To create His-tagged Ght, *ght* was amplified from pEN11-Ght with primers NMB0339-for and NMB0339-rev. The PCR product was cloned into pCRII-TOPO and subcloned into pEN11-Imp using NdeI/AatII restriction and ligation, yielding pEN11-His-Ght. The resulting plasmid encodes a fusion protein in which the first 38 amino acid residues of the Ght protein are replaced by a 6×His tag.

Primers lpxC-for-ndeI and lpxC-rev-aatII were used to amplify *lpxC* from genomic DNA of strain HB-1. The PCR product was digested with NdeI and AatII and ligated into similarly digested pEN11-Imp, resulting in pEN11-LpxC. Because we regularly experienced recombination events within the dual *lacUV5-tac* promoter present on pEN11 (4), we replaced this promoter with a single *tac* promoter. To this end, the *tac* promoter was amplified from pMMB67EH using primers tac-for and tac-rev. The resulting PCR product and pEN11 derivative pRIT16860 were digested with BglII and EcoRI and ligated together, yielding pEN25. Subsequently, the dual *lacUV5-tac* promoter was removed from pEN11-LpxC and replaced with the *tac* promoter from pEN25 using the BglII and NdeI restriction sites, resulting in pEN21-LpxC.

Primers lpxA-pEN-for and lpxA-pEN-rev were used to amplify *lpxA*

from genomic DNA of strain HB-1. The PCR product was ligated into pCRII-TOPO and subcloned into plasmid pEN11-Imp using NdeI and AatII, resulting in pEN11-LpxA.

To fuse Strep-tag II (WSHPQFEK) to LpxC, *lpxC* was amplified from HB-1 genomic DNA by using primers strep-lpxC-F and lpxC-rev-aatII, and the PCR product was cloned into pCRII-TOPO, resulting in pCRII-strep-*lpxC*. Next, the tagged *lpxC* gene was subcloned into pEN21 by AatII and NdeI restriction and ligation, yielding pEN21-Strep-LpxC.

For the deletion of *asmA*, the Kan^r cassette was cut from pMB25 with SacI and cloned into SacI-digested pUC21, resulting in plasmid pUC21-*kan*. DNA segments flanking *asmA* were amplified by PCR using primer pairs NMB1693-upF/NMB1693-upR and NMB1693-dnF/NMB1693-dnR and genomic DNA from strain HB-1 as the template and cloned into pUC21-*kan* using the restriction sites indicated in the primer sequences, resulting in pUC21-Δ*asmA*.

Construction of mutants. Neisserial strains were transformed by incubating cells with plasmids, restriction fragments, or PCR products on GC plates as described previously (26). An EcoRI fragment from pCRII-Δ*ght* was used to create Δ*ght* mutants. The deletion of *ght* in kanamycin-resistant transformants was confirmed by PCR using primers NMB0338-for and NMB0340-rev. The sizes of the resultant PCR fragments were taken as diagnostic for correct transformants, as wild-type and Δ*ght* mutant cells were expected to yield PCR products of 2,053 and 2,156 bp, respectively. For further verification, the PCR products were digested with BclI, which cuts only the wild-type PCR product.

HB-1Δ*asmA* was obtained by transformation of HB-1 with a PCR product produced from pUC21-Δ*asmA* with primers M13F and M13R. Kanamycin-resistant transformants were tested by PCR using primers NMB1693-upF and NMB1693-dnR, expected to yield 3,185- and 2,409-bp fragments for wild-type and Δ*asmA* mutant cells, respectively. Results were confirmed by PCR using primers asmAF and asmAR, which should give a 2,115-bp fragment in wild-type cells and no fragment in Δ*asmA* cells.

Since strains containing low LPS levels are poorly transformable (17, 27), most *ght* and *lptD* mutant strains containing plasmids were obtained by first transforming HB-1 with the corresponding plasmid and subsequently inactivating the chromosomal copy of *ght* or *lptD* by transformation with the appropriate inactivation construct in the presence of IPTG. We did succeed in obtaining HB-1Δ*ght*(pGht) by transforming HB-1Δ*ght* with pEN11-Ght.

Sensitivity assays. Sensitivity toward antibiotics was determined by plate assays using filter disks, as described previously (17). Heme sensitivity was similarly tested with a disk impregnated with 10 μl of a 5-mg/ml stock solution of hemin (Sigma).

Gel electrophoresis and immunoblotting. Sodium dodecyl sulfate-polyacrylamide gel electrophoresis (SDS-PAGE) and immunoblotting were performed as described previously (4, 28). LPS was analyzed as described previously (4). In brief, cells were boiled in SDS-PAGE sample buffer and treated with 0.5 mg/ml of proteinase K (Fermentas) for 1 h at 55°C. The resulting preparations were analyzed by SDS-PAGE on gels containing 14% acrylamide or by Tricine-SDS-PAGE (29) followed by staining with silver (30).

Antibodies. A polyclonal antiserum directed against alkaline phosphatase came from our laboratory stock (31). Monoclonal antibody SM1 directed against PilE was generously provided by John Heckels (University of Southampton). A monoclonal antibody directed against Strep-tag II was purchased from Novagen.

LPS localization assays. Accessibility of LPS in intact cells to extracellular neuraminidase (type V, *Clostridium perfringens*, catalog number N-2876; Sigma) or to intracellularly produced OM enzyme PagL was assessed as described previously (4).

Enzyme assays. Cells were grown on LB plates containing IPTG and arabinose for induction of the fusion proteins and supplemented with either 20 μg/ml of 5-bromo-4-chloro-3-indolyl-β-D-galactopyranoside (X-Gal) (Sigma) or 0.4 mg/ml of 5-bromo-4-chloro-3-indolylphosphate (XP) (Sigma) as the chromogenic substrate for β-galactosidase or alkaline phosphatase, respectively. Colony color was evaluated after incubation at 37°C overnight.

Separation of soluble and membrane proteins. Cell membranes of neisserial strains were isolated from ultrasonically disrupted cells by ultracentrifugation as described previously (32). Cell membranes from *E. coli* were isolated via the same procedure except that the ultracentrifugation step was extended from 5 min to 1 h. The soluble proteins were collected from the resulting supernatants by precipitation with 5% trichloroacetic acid (TCA).

LPS quantification. The 2-keto-3-deoxyoctonate (KDO) content of cell envelopes was measured as described previously (33).

Sequence analysis. To analyze the *pilE-lpxC* region on the chromosome, primers pilE-for and lpxC-dn-rev were designed based on the genome sequence of strain H44/76 (22) and used in a PCR with HiFi DNA polymerase (Roche Applied Science). The PCR fragments were cloned into pCRII-TOPO and sequenced by using primers M13F and M13R.

Quantitative real-time reverse transcription-PCR. Total RNA was isolated from bacteria grown in TSB by using TRIzol (Invitrogen) and further purified with Nucleospin RNA II columns (Macherey-Nagel). RNA was treated with Turbo DNA-Free (Ambion) to yield DNA-free RNA. cDNA was generated from 1 μg of RNA by using the Transcriptor High Fidelity cDNA synthesis kit (Roche). Quantitative real-time reverse transcription-PCR (qRT-PCR) was performed by using the 7900HT Fast real-time PCR system, SYBR green master mix (Applied Biosystems), and primers ermC-qPCR-for, ermC-qPCR-rev, lpxC-Fq, lpxC-Rq, omp85q-F, omp85q-R, rpmEq-F, and rpmEq-R (Table 3). Data analysis was performed by using the comparative cycle threshold method (Applied Biosystems) to determine relative expression levels. *ermC*, *omp85*, or *rpmE* transcript levels were used to normalize all data.

RESULTS

Phenotype of a *ght* mutant. To investigate the role of the Ght protein in *N. meningitidis*, we created a *ght* knockout mutation in strain HB-1, a nonencapsulated derivate of serogroup B strain H44/76. The Δ*ght* mutant showed an increased sensitivity to heme (Fig. 1A), confirming the previously reported *ght* mutant phenotype of another *N. meningitidis* strain (23). Also, in contrast to the parental strain, the Δ*ght* mutant was sensitive to vancomycin and showed a slightly increased sensitivity to tetracycline and chloramphenicol (Fig. 1A), consistent with a defect in the OM permeability barrier (17, 34). The sensitivity of the Δ*ght* mutant to hemin and the tested antibiotics was increased but to a lesser extent than observed for an *lpxA* mutant, which is defective in LPS synthesis (19), or an Δ*lptH* mutant, which is defective in LPS transport (Fig. 1A) (note that the *lptH* gene of *N. meningitidis* corresponds with *lptA* in *E. coli* [17]).

Interestingly, the mutant colonies had an opaque appearance compared to the more translucent colonies of the parental strain (data not shown). This feature had been observed previously in mutant strains compromised in LPS biogenesis (4). Also, similar to LPS biosynthesis and transport mutants (4, 17, 35), the Δ*ght* mutant showed a reduced growth rate (Fig. 1B). Because of its resemblance to strains producing low levels of LPS, we next assessed the total cellular amount of LPS in the Δ*ght* mutant by SDS-PAGE and found it to be severely reduced (Fig. 1C). The reduction in cellular LPS could be complemented by introducing a plasmid carrying a wild-type copy of *ght* (Fig. 1C). The reduced cellular LPS content was confirmed by measuring the amount of 2-keto-3-deoxyoctonate (KDO), a sugar found almost exclusively in LPS. These measurements showed that the cell envelopes of the mutant contained only 15% of the wild-type LPS levels. Thus, the Ght protein is involved in LPS biogenesis by affecting LPS biosyn-

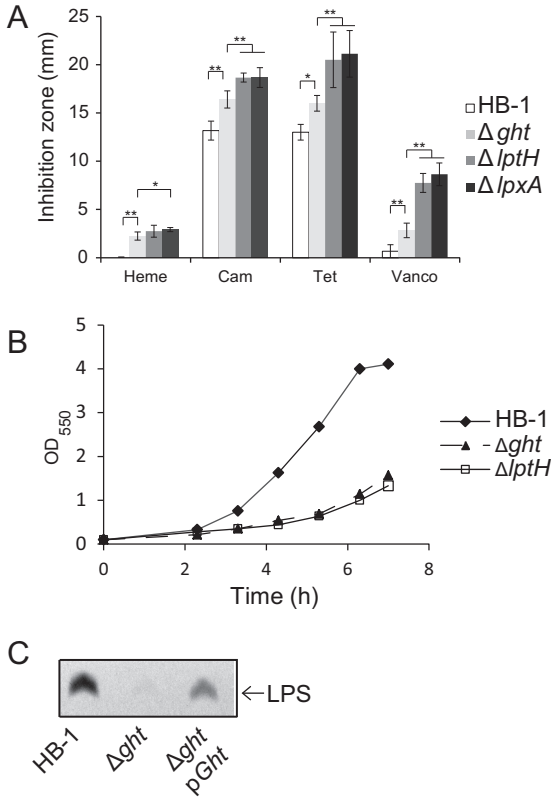

FIG 1 Phenotypes of a Δ*ght* mutant. (A) Strains indicated at the right were grown overnight on nonselective plates with filter disks containing either 50 μg of heme, 30 μg of vancomycin (Vanco), 10 μg of tetracycline (Tet), or 5 μg of chloramphenicol (Cam). Growth inhibition zones were measured in millimeters from the rim of the disk. Statistical analysis was done by a one-way analysis of variance followed by a *post hoc* Bonferroni test. Significant differences are indicated by ∗ ($P < 0.05$) or ∗∗ ($P < 0.005$). (B) Growth of strain HB-1 and its Δ*ght* mutant derivative in TSB was monitored by measuring the optical density at 550 nm (OD_{550}). For comparison, the growth curve of an Δ*lptH* mutant, which is affected in LPS transport, is also shown. (C) LPS levels in equal amounts (on the basis of the optical density at 550 nm) of proteinase K-treated whole-cell lysates of the indicated strains were assessed by SDS-PAGE followed by staining with silver. The Δ*ght*(pGht) strain was grown in the presence of IPTG.

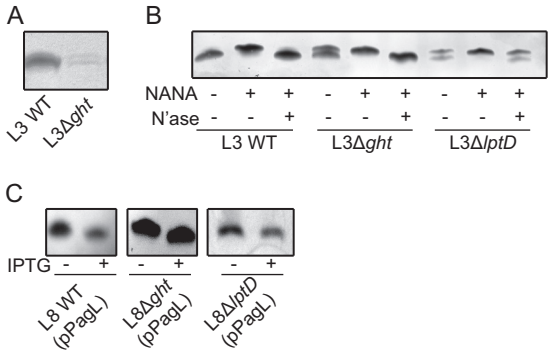

FIG 2 LPS is transported to the cell surface in the Δ*ght* mutant. Cells lysates were processed for Tricine-SDS-PAGE followed by silver staining of LPS. In panel A, equal amounts of cells were loaded, while in panels B and C, the cell lysates of the Δ*ght* and Δ*lptD* mutants were overloaded relative to the wild type (WT) to improve visualization of the LPS. (A) LPS contents of wild-type strain H44/76 immunotype L3 and its Δ*ght* derivative. (B) Strain H44/76 L3 and its Δ*ght* and Δ*lptD* derivatives were grown in the presence of CMP-NANA (NANA), and intact cells were either treated or not with neuraminidase (N′ase), as indicated. Note that the LPS in the two mutant strains was already partially sialylated even when grown without CMP-NANA, as observed previously (4). (C) Strain H44/76 immunotype L8 and its Δ*ght* and Δ*lptD* derivatives, all containing an IPTG-inducible copy of *pagL* on a plasmid, were grown in the presence (+) or absence (−) of IPTG.

thesis or, alternatively, LPS transport, since LPS transport defects in *N. meningitidis* also result in decreased LPS levels (4, 17, 20).

Localization of LPS. To assess whether Ght is involved in LPS transport, we determined if the residual amounts of LPS produced in the mutant are transported to the cell surface. To this end, we made use of a previously established method based on determining the accessibility of sialylated LPS in intact cells to extracellular neuraminidase (4). LPS of strain HB-1 is truncated due to a *galE* mutation and therefore cannot be sialylated. Hence, we first introduced the Δ*ght* mutation into an H44/76 strain of immunotype L3, which can be fully sialylated when the strain is grown on CMP-NANA (4). As in the Δ*ght* derivative of HB-1, the LPS content in the Δ*ght* mutant of strain H44/76 was severely decreased (Fig. 2A). Neuraminidase treatment of intact wild-type cells producing sialylated LPS increased the electrophoretic mobility of the LPS, consistent with the removal of the sialic acid residue (Fig. 2B). In a Δ*lptD* mutant strain, where LPS is not present at the cell surface due to a defect in LPS transport, similar treatment left most of the LPS intact (Fig. 2B). In contrast, in Δ*ght* mutant cells, the residual LPS produced was completely converted into the faster-migrating form (Fig. 2B), demonstrating that the LPS was accessible to neuraminidase and therefore normally transported to the bacterial cell surface.

The correct localization of LPS in a Δ*ght* mutant was further verified in another assay that is based on the integral OM-embedded enzyme PagL. This enzyme removes an acyl chain from LPS, only when LPS is present in the outer leaflet of the OM (4). We deleted the *ght* gene in the previously constructed H44/76 strain of immunotype L8 carrying the *pagL* gene from *Bordetella bronchiseptica* under the control of an IPTG-inducible promoter on a plasmid (4). Induction of PagL synthesis in the parent strain increased the electrophoretic mobility of the LPS (Fig. 2C), consistent with the removal of an acyl chain, whereas this was not the case for the same strain carrying an *lptD* deletion (Fig. 2C). Induction of PagL synthesis in the Δ*ght* mutant resulted in faster-migrating LPS, similar to the parent strain (Fig. 2C), confirming the proper localization of LPS in the Δ*ght* mutant. Together, these results demonstrate that Ght is not required for LPS transport but apparently plays a role in LPS biosynthesis or the regulation thereof. Since all LPS biosynthetic enzymes are known, a regulatory role for Ght appears most probable.

Localization and topology of Ght. To understand at what level of the LPS biogenesis process Ght might act, we investigated its localization and topology. Inspection of the sequence of Ght showed that it contains an N-terminal hydrophobic segment, six tetratricopeptide repeat (TPR) domains, and a putative C4-type zinc finger or zinc-binding domain (Fig. 3A) (23). Previously, the N-terminal hydrophobic sequence was suggested to function as a periplasmic targeting signal (23). However, we noticed that the hydrophobic stretch is flanked by negatively charged residues toward the N terminus and positively charged residues at the C-terminal end (Fig. 3A). This charge distribution is conserved in Ght

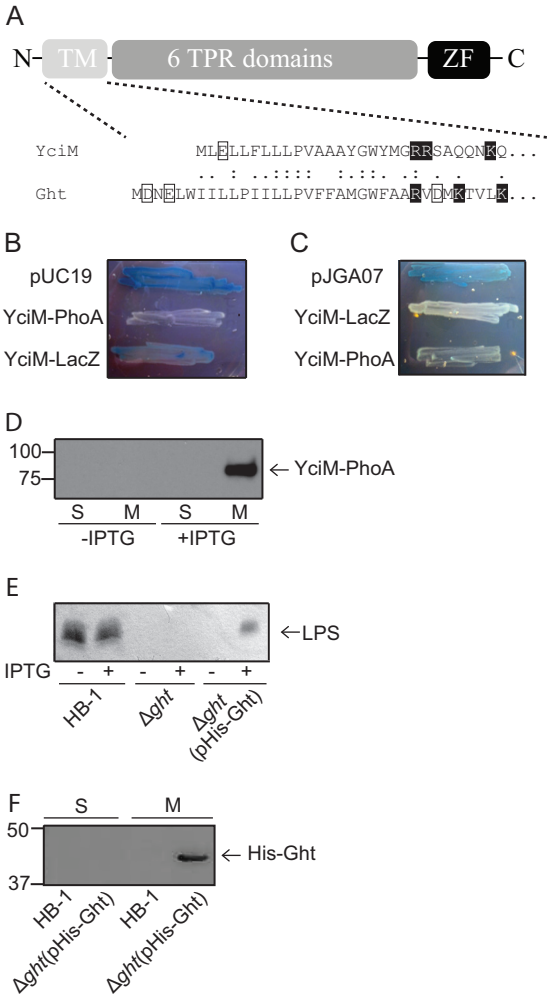

FIG 3 Localization and topology of YciM and Ght. (A) Protein domain prediction. TM, transmembrane domain; TPR, tetratricopeptide repeat; ZF, zinc finger. Amino acid sequences of the TM domains of YciM and Ght are aligned, with similar amino acid residues indicated with periods and identical residues indicated with colons. Negatively and positively charged residues are indicated by open and black boxes, respectively. (B) Strains were grown on a plate containing the chromogenic β-galactosidase substrate X-Gal. From top to bottom, cultures of DH5α containing pUC19 (positive control), pBAD*yciM-phoA* (negative control), and pBAD*yciM-lacZ* are shown. (C) Strains were grown on a plate containing the chromogenic PhoA substrate XP. From top to bottom, cultures of DH5α containing pJGA07 (positive control), pBAD*yciM-lacZ* (negative control), and pBAD*yciM-phoA* are shown. (D) DH5α containing pBAD*yciM-phoA* was grown in the presence or absence of IPTG. Membrane fractions (M) and soluble proteins (S) were isolated and analyzed by SDS-PAGE and immunoblotting with an antiserum directed against PhoA. (E) LPS contents of HB-1, HB-1Δ*ght*, and HB-1Δ*ght*(pHis-Ght). Cells were grown in the presence or absence of IPTG. Equal amounts of cells (on the basis of the optical density at 550 nm) were processed for LPS analysis by SDS-PAGE. (F) HB-1 and HB-1Δ*ght*(pHis-Ght) were grown in the presence of IPTG. Membrane fractions (M) and soluble proteins (S) were isolated and analyzed by SDS-PAGE and immunoblotting with an anti-6×His antibody. Molecular weight (in thousands) is indicated on the left.

homologs from other bacteria, such as YciM from *E. coli* (Fig. 3A). Therefore, based on the positive-inside rule (36), we hypothesized that the hydrophobic domain of Ght could function as an IM anchor, resulting in an N_{out}-C_{in} topology with the major part of the protein located in the cytoplasm.

Since protocols for studying the topology of membrane proteins using reporter fusions have been well established in *E. coli*, we decided to analyze the topology of the Ght homolog YciM in *E. coli*. To determine Ght topology, we constructed fusions with a β-galactosidase fragment (LacZα) or alkaline phosphatase (PhoA) to the C terminus of YciM. PhoA will be active only in the periplasm since it requires disulfide bridge formation, while the LacZ moiety will show activity only in the cytoplasm since it requires complementation with the LacZΩ moiety present in this cellular compartment. When DH5α cells synthesizing the YciM-LacZα fusion protein were grown on plates containing the chromogenic β-galactosidase substrate X-Gal, we observed β-galactosidase activity, indicating that LacZα was located in the cytoplasm (Fig. 3B). LacZα, expressed from pUC19 in DH5α, served as a positive control for this assay (Fig. 3B, top streak). Conversely, when cells producing the YciM-PhoA fusion protein were grown on plates containing the PhoA substrate XP, we did not observe phosphatase activity, indicating that the PhoA moiety of the protein was not exported to the periplasm (Fig. 3C). The positive control for this assay was provided by expression of the fusion protein XcpT-PhoA (37) (Fig. 3C, top streak). Production and membrane localization of the chimeric YciM-PhoA protein were confirmed by immunoblotting with an antiserum directed against PhoA (Fig. 3D).

To verify if Ght of *N. meningitidis* functions in the cytoplasm, strain HB-1Δ*ght*(pHis-Ght) was constructed. This strain produces a mutant Ght protein with a 6×His tag replacing the N-terminal membrane anchor from a plasmid. This deletion should prevent transport of the protein to the periplasm or its insertion into the IM. In the absence of IPTG, these cells produced very little LPS, as expected. However, upon the addition of IPTG, an increase in the total amount of LPS was observed, indicating that the mutant Ght protein is able to complement, at least partially, the lack of wild-type Ght (Fig. 3E). Additionally, we observed that the growth rate, sensitivity to vancomycin, and sensitivity to tetracycline were also partially restored (data not shown). Next, we determined the subcellular localization of the mutant Ght protein. Surprisingly, His-tagged Ght without the membrane anchor was still found in the membrane fraction (Fig. 3F). Together, these results indicate that the N-terminal hydrophobic domain of YciM, and therefore probably also that of its homolog Ght, functions as a membrane anchor with an N_{out}-C_{in} topology, while the major part of the protein is located in the cytoplasm. However, the cytoplasmic domain alone appears to be sufficient for function and is still targeted to the membrane, presumably via protein-protein interactions.

Characterization of Δ*ght* pseudorevertants. Interestingly, we noticed occasionally upon subculturing of *ght* mutant strains the growth of colonies with a wild-type-like translucent appearance. These colonies could not represent true revertants, since the constructed *ght* mutation is a deletion of almost the entire *ght* coding region. Indeed, bacteria from the translucent colonies were still resistant to kanamycin, and PCR analyses confirmed that they still lacked the *ght* gene. We decided to study these pseudorevertants since the identification of the suppressor mutations was anticipated to provide insight into the role of Ght in LPS biogenesis. Two independently obtained pseudorevertants, HB-1Δ*ght-rev1* and HB-1Δ*ght-rev2*, were studied in detail. Analysis of their LPS content by SDS-PAGE revealed that they produced wild-type lev-

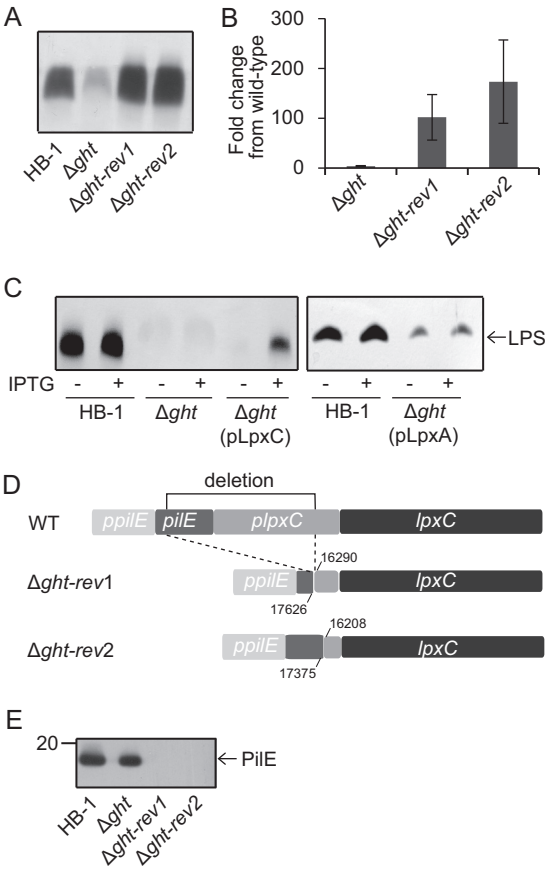

FIG 4 Analysis of pseudorevertants of the Δ*ght* mutant. (A) Strain HB-1, its Δ*ght* mutant derivative, and two independently obtained pseudorevertants of the Δ*ght* mutant were grown in TSB and processed for LPS analysis by SDS-PAGE and staining with silver. (B) Total RNA from cells grown in TSB was harvested and used to make cDNA. The amounts of *lpxC* transcripts were determined by qRT-PCR. Expression levels are depicted as fold changes compared to the transcript levels in HB-1 cells. Shown are the average results of three independent experiments, each normalized to the amounts of three different transcripts, i.e., *ermC*, *omp85*, and *rpmE*. The error bars depict the standard errors of the means. (C) HB-1, HB-1Δ*ght*, and HB-1Δ*ght* containing pEN21-LpxC or pEN11-LpxA were grown in the absence or presence of IPTG, as indicated, and processed for LPS analysis by SDS-PAGE followed by staining with silver. (D) Schematic representation of the genetic regions containing the *lpxC* gene. Intergenic regions containing the promoters of *pilE* and *lpxC* are indicated as *ppilE* and *plpxC*, respectively. The extents of the deletions found in the pseudorevertants, which place the *lpxC* gene behind the *pilE* promoter, are indicated. The genomic positions (based on the genome sequence of strain H44/76 [22]) of the start and end of each deletion are indicated. (E) Immunoblot showing cellular PilE levels. Molecular weight (in thousands) is indicated on the left. In panels A, C, and E, equal numbers of cells, based on measurements of the optical density at 550 nm, were loaded.

els of LPS (Fig. 4A), consistent with their translucent-colony phenotype.

In *E. coli*, LpxC catalyzes the rate-limiting step in LPS synthesis, and its levels are carefully controlled at the posttranscriptional level (38–40). Hence, we considered the possibility that Ght regulates LpxC activity in *N. meningitidis* and that its absence can be compensated for by *lpxC* overexpression. We tested this possibility by measuring the *lpxC* transcription levels by qRT-PCR. Indeed, we found a drastic increase in *lpxC* transcription levels in both pseudorevertants relative to wild-type levels (Fig. 4B). The

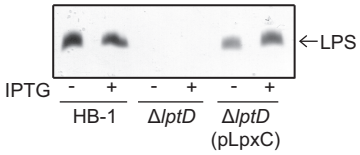

FIG 5 Restoration of LPS production in an LPS transport mutant by LpxC overproduction. Cells of HB-1, HB-1Δ*lptD*, and HB-1Δ*lptD* containing *lpxC* behind an IPTG-inducible promoter on pEN21-LpxC were grown in TSB in the presence or absence of IPTG, as indicated. Equal amounts of cells were processed for LPS analysis by SDS-PAGE, followed by staining of LPS with silver.

lpxC mRNA levels in the Δ*ght* mutant were only marginally increased relative to those in HB-1 (Fig. 4B), as was also observed for HB-1Δ*ght*(pGht) (data not shown), suggesting that Ght does not regulate *lpxC* expression. The notion that the Δ*ght* mutation could be compensated for by increased *lpxC* expression levels was confirmed by the observation that artificial overproduction of LpxC in a Δ*ght* strain from a plasmid containing *lpxC* under *tac* promoter control partially restored LPS production (Fig. 4C, left). In contrast, overproduction of LpxA, the first enzyme involved in LPS synthesis, did not result in a similar restoration of LPS levels (Fig. 4C, right), suggesting that the compensatory effect on the *ght* mutation is specific for LpxC.

Next, we set out to identify the nature of the suppressor mutations in the pseudorevertants. We anticipated finding mutations in the *lpxC* promoter region, but several attempts to amplify this region from the mutants by PCR with different primer sets failed, suggesting that serious rearrangements had occurred. Eventually, with a forward primer annealing near the 5′ end of the upstream-located *pilE* gene and a reverse primer in the coding region of *lpxC*, we obtained a PCR product from both pseudorevertants, which was, however, considerably smaller than the corresponding product obtained from the wild-type strain or the Δ*ght* mutant. Sequencing of the PCR products revealed that in both cases, a deletion had occurred which removed a part of *pilE* and a part of the downstream intergenic region containing the *lpxC* promoter (Fig. 4D). These deletions would result in expression of *lpxC* from the *pilE* promoter, which is constitutively expressed, presumably at a very high level, since *pilE* encodes the major structural subunit of the type IV pili. The anticipated lack of PilE production in the pseudorevertants was confirmed by immunoblotting (Fig. 4E).

Restoration of LPS production in an *lptD* mutant by LpxC overproduction. Like the Δ*ght* mutant, all meningococcal LPS transport mutants produce severely reduced amounts of LPS (4, 17, 20), indicating the existence of a negative feedback mechanism upon LPS synthesis when transport fails. We hypothesize that Ght is implicated in this feedback mechanism. Since the defect in LPS synthesis in the Δ*ght* mutant could be overcome by overproducing LpxC, we considered the possibility that the negative feedback inhibition of LPS synthesis in an LPS transport mutant could also be bypassed by LpxC overproduction. Indeed, the levels of LPS in an *lptD* mutant of strain HB-1 were partially restored when LpxC was expressed from plasmid pEN21-LpxC (Fig. 5). The partial restoration of LPS synthesis observed in the absence of IPTG could be due to leaky expression from the single *tac* promoter on the plasmid.

Interaction between Ght and LpxC. The predicted presence of TPR and zinc finger domains in Ght is suggestive of an involve-

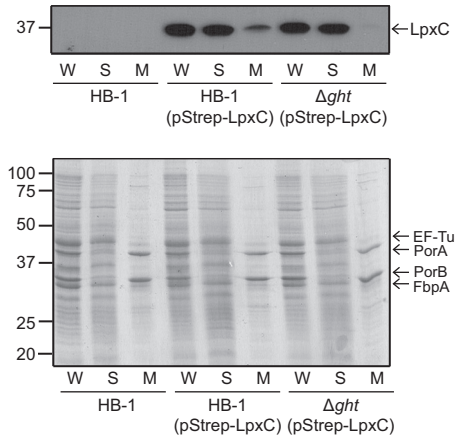

FIG 6 Ght tethers LpxC to the membrane. Strains HB-1, HB-1(pStrep-LpxC), and HB-1Δ*ght*(pStrep-LpxC) were grown in the presence of IPTG. Whole cells (W) were separated into soluble proteins (S) and a membrane fraction (M). The obtained fractions were subjected to SDS-PAGE and immunoblot analysis using an antibody directed against Strep-tag II (top) or were subjected to SDS-PAGE and Coomassie staining for a loading control (bottom). The positions of the cytoplasmic marker EF-Tu, the OM proteins PorA and PorB, and the periplasmic marker FbpA are indicated. Molecular weight (in thousands) is indicated on the left.

ment of Ght in protein-protein interactions. We hypothesized that Ght might affect the level or activity of the LpxC protein, possibly by a direct interaction between the two proteins. If LpxC binds Ght, LpxC should also be associated with the inner membrane, even though it is a soluble protein. To investigate this possibility, we attached an N-terminal Strep-tag II to LpxC (Strep-LpxC). The Strep-tag II-tagged LpxC protein was expressed in wild-type and Δ*ght* mutant strains. Subsequently, cells were harvested and lysed, and the membranes were separated from the soluble proteins. In the presence of Ght, Strep-LpxC was found in both the soluble and the membrane fractions (Fig. 6) despite its lack of a hydrophobic membrane anchor. However, in the absence of Ght, all Strep-LpxC was present in the soluble fraction (Fig. 6), indicating that Ght tethers LpxC to the IM.

AsmA has no significant role in LPS biogenesis in *N. meningitidis*. In a high-throughput screen linking growth profiles of *E. coli* under different conditions to specific mutations, a link between the homolog of *ght*, i.e., *yciM*, and *asmA* was suggested (41). The *asmA* gene in *E. coli* was initially discovered in suppressor mutants allowing OM insertion of an otherwise assembly-defective OmpF protein (42). Interestingly, deletion of this gene in *E. coli* led to a decrease in the amount of LPS (43). Therefore, we investigated whether AsmA also has a role in LPS biogenesis in *N. meningitidis*. To this end, we deleted the homologous locus (locus tag NMH_1332 in the genome sequence of H44/76, which corresponds to locus tag NMB1693 in the genome sequence of MC58) in strain HB-1. The resulting Δ*asmA* mutant was indistinguishable from its parent in growth rate, LPS levels measured by SDS-PAGE, and sensitivity to ampicillin, vancomycin, and novobiocin (data not shown). Hence, the AsmA protein has no apparent role in LPS biogenesis in *N. meningitidis*.

DISCUSSION

We identified the Ght protein as a novel regulator of LPS biosynthesis in *N. meningitidis*. While it was previously suggested that Ght is a periplasmic protein (23), we show here that Ght is in fact an N-terminally anchored IM protein, with the major part of the protein being located in the cytoplasm. This topology is supported by the observation that a truncated Ght protein lacking the N-terminal membrane anchor is able to complement a Δ*ght* mutant. Interestingly, we found that high-level overexpression of *lpxC*, which encodes the enzyme that catalyzes the first committed step in LPS synthesis (3), compensates for the absence of Ght. Being located at the cytoplasmic side of the IM, Ght could potentially interact directly with LpxC.

Based on our results, we propose a model in which Ght is part of a control mechanism that senses the accumulation of LPS in the IM when LPS transport is compromised. Sensing of LPS accumulation then alters the conformation of Ght, which affects the activity of the LpxC enzyme. A possible role of Ght in the feedback inhibition of LPS synthesis when LPS transport is hampered is supported by our finding that the decreased LPS content in an LptD-deficient strain, as in a Δ*ght* mutant, can be overcome by inducing high levels of LpxC. However, the exact mechanism by which Ght influences LpxC activity remains to be clarified. Possibly, LpxC functions most efficiently when it is tethered to the IM, as mediated by Ght. Obviously, the absence of Ght could be compensated for in such cases by LpxC overproduction. Alternatively, Ght could protect LpxC from proteolytic degradation. LpxC catalyzes the rate-limiting step in lipid A biosynthesis (3). In *E. coli*, this step was shown to be regulated by FtsH-mediated proteolysis of LpxC, which requires a specific signal (LAXXXXXAVLA) at the C terminus of LpxC (38–40). This signal is not present at the C terminus of meningococcal LpxC. However, FtsH is not always responsible for the turnover of LpxC. In *Agrobacterium tumefaciens* and *Rhodobacter capsulatus*, LpxC can be degraded by the protease Lon, while *Pseudomonas aeruginosa* employs an unknown, proteolysis-independent strategy to control its LPS content (39). Hence, whether LpxC of *N. meningitidis* is a target for proteolysis and, if so, to which proteolytic enzyme remain to be determined.

Homologs of Ght are found in many other, although not all, proteobacteria (23), mostly in those belonging to the beta- and gammaproteobacterial species, such as, for example, *Burkholderia*, *Yersinia*, *Vibrio*, *Salmonella*, *Coxiella*, and *Haemophilus* species. Thus, a Ght-mediated regulatory mechanism controlling LPS biosynthesis may be widespread. In *E. coli*, the *ght* homolog *yciM* was first identified as a gene involved in biofilm formation (44). It was reported that a *yciM* mutant had a decreased content of OM proteins (44). Since the proper assembly of a number of OM proteins in *E. coli* depends on LPS (43, 45), this phenotype of the *yciM* mutant could reflect an LPS biogenesis defect. Furthermore, an increased sensitivity toward antibiotics such as novobiocin, which was observed for the *yciM* mutant (44), was also found for *E. coli* mutants defective in LPS biogenesis (5). Interestingly, *E. coli* appears to respond to a defect in LPS transport by increasing LPS synthesis (6), as opposed to the decrease observed in *N. meningitidis*. Thus, although both organisms appear to sense defects in LPS transport, which may be mediated by the conserved component(s) of the regulatory system, the response is different, which may be reflected in a different proteolytic control of LpxC activity, as discussed above. Studies of both organisms are clearly warranted to fully understand the regulatory mechanism that controls LPS biosynthesis.

In meningococcal genome sequences, the *ght* gene is preceded

by a open reading frame (ORF) (locus tags NMH_1912 and NMB0338 in the genome sequences of H44/76 [22] and MC58 [21], respectively) potentially encoding a small (104 amino acids in the case of H44/76 and N-terminally extended by 56 residues in the case of MC58, presumably due to the incorrect assignment of the start codon) conserved membrane protein of unknown function (DUF1049) with two membrane-spanning segments. As the stop codon of this ORF is separated by only 10 bp from the start codon of *ght*, the two genes likely constitute an operon. Analysis of genome sequences at the NCBI revealed the presence of an ORF encoding a similar membrane protein upstream of the *ght* homolog in many proteobacteria (data not shown); for example, its homolog in *E. coli* is designated *yciS*. Interestingly, BLAST searches also identified genes encoding proteins that combine a DUF1049 domain at the N terminus with a Ght/YciM-like domain at the C terminus, e.g., the gene with locus tag NITGR_260009 of *Nitrospina gracilis* 3/211. Therefore, it seems likely that Ght forms a complex with the IM protein encoded by the upstream ORF and that they function together in signaling and responding to LPS accumulating in the IM. The formation of such a complex could explain why a mutant Ght protein lacking its N-terminal membrane anchor was still found associated with the membrane. The possible involvement of this IM protein in the regulation of LPS biosynthesis and its interaction with Ght will have to be established and are our next goals.

ADDENDUM

While the manuscript was under revision, a manuscript by Mahalakshmi et al. reporting that YciM in *E. coli* may modulate the proteolytic activity of FtsH toward LpxC was accepted for publication (46). It is noteworthy that inactivation of *yciM* in *E. coli* resulted in overproduction of LPS (46), while we demonstrate in this paper that inactivation of *ght* in *N. meningitidis* drastically reduces LPS synthesis, thus reflecting the different responses of these organisms to defects in LPS transport (4, 6).

REFERENCES

1. **Polissi A, Georgopoulos C.** 1996. Mutational analysis and properties of the *msbA* gene of *Escherichia coli*, coding for an essential ABC family transporter. Mol. Microbiol. **20:**1221–1233. http://dx.doi.org/10.1111/j.1365-2958.1996.tb02642.x.
2. **Zhou Z, White KA, Polissi A, Georgopoulos C, Raetz CRH.** 1998. Function of *Escherichia coli* MsbA, an essential ABC family transporter, in lipid A and phospholipid biosynthesis. J. Biol. Chem. **273:**12466–12475. http://dx.doi.org/10.1074/jbc.273.20.12466.
3. **Raetz CRH, Whitfield C.** 2002. Lipopolysaccharide endotoxins. Annu. Rev. Biochem. **71:**635–700. http://dx.doi.org/10.1146/annurev.biochem.71.110601.135414.
4. **Bos MP, Tefsen B, Geurtsen J, Tommassen J.** 2004. Identification of an outer membrane protein required for the transport of lipopolysaccharide to the bacterial cell surface. Proc. Natl. Acad. Sci. U. S. A. **101:**9417–9422. http://dx.doi.org/10.1073/pnas.0402340101.
5. **Ruiz N, Gronenberg LS, Kahne D, Silhavy TJ.** 2008. Identification of two inner-membrane proteins required for the transport of lipopolysaccharide to the outer membrane of *Escherichia coli*. Proc. Natl. Acad. Sci. U. S. A. **105:**5537–5542. http://dx.doi.org/10.1073/pnas.0801196105.
6. **Sperandeo P, Cescutti R, Villa R, Di Benedetto C, Candia D, Dehò G, Polissi A.** 2007. Characterization of *lptA* and *lptB*, two essential genes implicated in lipopolysaccharide transport to the outer membrane of *Escherichia coli*. J. Bacteriol. **189:**244–253. http://dx.doi.org/10.1128/JB.01126-06.
7. **Sperandeo P, Lau FK, Carpentieri A, De Castro C, Molinaro A, Dehò G, Silhavy TJ, Polissi A.** 2008. Functional analysis of the protein machinery required for transport of lipopolysaccharide to the outer membrane of *Escherichia coli*. J. Bacteriol. **190:**4460–4469. http://dx.doi.org/10.1128/JB.00270-08.
8. **Wu T, McCandlish AC, Gronenberg LS, Chng SS, Silhavy TJ, Kahne D.** 2006. Identification of a protein complex that assembles lipopolysaccharide in the outer membrane of *Escherichia coli*. Proc. Natl. Acad. Sci. U. S. A. **103:**11754–11759. http://dx.doi.org/10.1073/pnas.0604744103.
9. **Chng SS, Gronenberg LS, Kahne D.** 2010. Proteins required for lipopolysaccharide assembly in *Escherichia coli* form a transenvelope complex. Biochemistry **49:**4565–4567. http://dx.doi.org/10.1021/bi100493e.
10. **Narita S, Tokuda H.** 2009. Biochemical characterization of an ABC transporter LptBFGC complex required for the outer membrane sorting of lipopolysaccharides. FEBS Lett. **583:**2160–2164. http://dx.doi.org/10.1016/j.febslet.2009.05.051.
11. **Okuda S, Freinkman E, Kahne D.** 2012. Cytoplasmic ATP hydrolysis powers transport of lipopolysaccharide across the periplasm in *E. coli*. Science **338:**1214–1217. http://dx.doi.org/10.1126/science.1228984.
12. **Chng SS, Ruiz N, Chimalakonda G, Silhavy TJ, Kahne D.** 2010. Characterization of the two-protein complex in *Escherichia coli* responsible for lipopolysaccharide assembly at the outer membrane. Proc. Natl. Acad. Sci. U. S. A. **107:**5363–5368. http://dx.doi.org/10.1073/pnas.0912872107.
13. **Ruiz N, Chng SS, Hiniker A, Kahne D, Silhavy TJ.** 2010. Nonconsecutive disulfide bond formation in an essential integral outer membrane protein. Proc. Natl. Acad. Sci. U. S. A. **107:**12245–12250. http://dx.doi.org/10.1073/pnas.1007319107.
14. **Chimalakonda G, Ruiz N, Chng SS, Garner RA, Kahne D, Silhavy TJ.** 2011. Lipoprotein LptE is required for the assembly of LptD by the β-barrel assembly machine in the outer membrane of *Escherichia coli*. Proc. Natl. Acad. Sci. U. S. A. **108:**2492–2497. http://dx.doi.org/10.1073/pnas.1019089108.
15. **Grabowicz M, Yeh J, Silhavy TJ.** 2013. Dominant negative *lptE* mutation that supports a role for LptE as a plug in the LptD barrel. J. Bacteriol. **195:**1327–1334. http://dx.doi.org/10.1128/JB.02142-12.
16. **Freinkman E, Chng SS, Kahne D.** 2011. The complex that inserts lipopolysaccharide into the bacterial outer membrane forms a two-protein plug-and-barrel. Proc. Natl. Acad. Sci. U. S. A. **108:**2486–2491. http://dx.doi.org/10.1073/pnas.1015617108.
17. **Bos MP, Tommassen J.** 2011. The LptD chaperone LptE is not directly involved in lipopolysaccharide transport in *Neisseria meningitidis*. J. Biol. Chem. **286:**28688–28696. http://dx.doi.org/10.1074/jbc.M111.239673.
18. **Tefsen B, Geurtsen J, Beckers F, Tommassen J, de Cock H.** 2005. Lipopolysaccharide transport to the bacterial outer membrane in spheroplasts. J. Biol. Chem. **280:**4504–4509. http://dx.doi.org/10.1074/jbc.M409259200.
19. **Steeghs L, den Hartog R, den Boer A, Zomer B, Roholl P, van der Ley P.** 1998. Meningitis bacterium is viable without endotoxin. Nature **392:**449–450. http://dx.doi.org/10.1038/33046.
20. **Tefsen B, Bos MP, Beckers F, Tommassen J, de Cock H.** 2005. MsbA is not required for phospholipid transport in *Neisseria meningitidis*. J. Biol. Chem. **280:**35961–35966. http://dx.doi.org/10.1074/jbc.M509026200.
21. **Tettelin H, Saunders NJ, Heidelberg J, Jeffries AC, Nelson KE, Eisen JA, Ketchum KA, Hood DW, Peden JF, Dodson RJ, Nelson WC, Gwinn ML, DeBoy R, Peterson JD, Hickey EK, Haft DH, Salzberg SL, White O, Fleischmann RD, Dougherty BA, Mason T, Ciecko A, Parksey DS, Blair E, Cittone H, Clark EB, Cotton MD, Utterback TR, Khouri H, Qin H, Vamathevan J, Gill J, Scarlato V, Masignani V, Pizza M, Grandi G, Sun L, Smith HO, Fraser CM, Moxon ER, Rappuoli R, Venter JC.** 2000. Complete genome sequence of *Neisseria meningitidis* serogroup B strain MC58. Science **287:**1809–1815. http://dx.doi.org/10.1126/science.287.5459.1809.
22. **Piet JR, Huis in't Veld RAG, van Schaik BDC, van Kampen AHC, Baas F, van de Beek D, Pannekoek Y, van der Ende A.** 2011. Genome sequence of *Neisseria meningitidis* serogroup B strain H44/76. J. Bacteriol. **193:**2371–2372. http://dx.doi.org/10.1128/JB.01331-10.
23. **Rasmussen AW, Alexander HL, Perkins-Balding D, Shafer WM, Stojiljkovic I.** 2005. Resistance of *Neisseria meningitidis* to the toxic effects of heme iron and other hydrophobic agents requires expression of *ght*. J. Bacteriol. **187:**5214–5223. http://dx.doi.org/10.1128/JB.187.15.5214-5223.2005.
24. **Blattner FR, Plunkett G, III, Bloch CA, Perna NT, Burland V, Riley M, Collado-Vides J, Glasner JD, Rode CK, Mayhew GF, Gregor J, Davis NW, Kirkpatrick HA, Goeden MA, Rose DJ, Mau B, Shao Y.** 1997. The complete genome sequence of *Escherichia coli* K-12. Science **277:**1453–1462. http://dx.doi.org/10.1126/science.277.5331.1453.

25. **Wilson K.** 2001. Preparation of genomic DNA from bacteria. Curr. Protoc. Mol. Biol. Chapter 2:Unit 2.4. http://dx.doi.org/10.1002/0471142727.mb0204s56.
26. **van Dam V, Bos MP.** 2012. Generating knock-out and complementation strains of *Neisseria meningitidis*. Methods Mol. Biol. **799:**55–72. http://dx.doi.org/10.1007/978-1-61779-346-2_4.
27. **Albiger B, Johansson L, Jonsson AB.** 2003. Lipooligosaccharide-deficient *Neisseria meningitidis* shows altered pilus-associated characteristics. Infect. Immun. **71:**155–162. http://dx.doi.org/10.1128/IAI.71.1.155-162.2003.
28. **Laemmli UK.** 1970. Cleavage of structural proteins during the assembly of the head of bacteriophage T4. Nature **227:**680–685. http://dx.doi.org/10.1038/227680a0.
29. **Lesse AJ, Campagnari AA, Bittner WE, Apicella MA.** 1990. Increased resolution of lipopolysaccharides and lipooligosaccharides utilizing Tricine-sodium dodecyl sulfate-polyacrylamide gel electrophoresis. J. Immunol. Methods **126:**109–117. http://dx.doi.org/10.1016/0022-1759(90)90018-Q.
30. **Tsai CM, Frasch CE.** 1982. A sensitive silver stain for detecting lipopolysaccharides in polyacrylamide gels. Anal. Biochem. **119:**115–119. http://dx.doi.org/10.1016/0003-2697(82)90673-X.
31. **Scholten M, Janssen R, Bogaarts C, van Strien J, Tommassen J.** 1995. The *pho* regulon of *Shigella flexneri*. Mol. Microbiol. **15:**247–254. http://dx.doi.org/10.1111/j.1365-2958.1995.tb02239.x.
32. **Voulhoux R, Bos MP, Geurtsen J, Mols M, Tommassen J.** 2003. Role of a highly conserved bacterial protein in outer membrane protein assembly. Science **299:**262–265. http://dx.doi.org/10.1126/science.1078973.
33. **Karkhanis YD, Zeltner JY, Jackson JJ, Carlo DJ.** 1978. A new and improved microassay to determine 2-keto-3-deoxyoctonate in lipopolysaccharide of Gram-negative bacteria. Anal. Biochem. **85:**595–601. http://dx.doi.org/10.1016/0003-2697(78)90260-9.
34. **Sampson BA, Misra R, Benson SA.** 1989. Identification and characterization of a new gene of *Escherichia coli* K-12 involved in outer membrane permeability. Genetics **122:**491–501.
35. **Steeghs L, de Cock H, Evers E, Zomer B, Tommassen J, van der Ley P.** 2001. Outer membrane composition of a lipopolysaccharide-deficient *Neisseria meningitidis* mutant. EMBO J. **20:**6937–6945. http://dx.doi.org/10.1093/emboj/20.24.6937.
36. **von Heijne G, Gavel Y.** 1988. Topogenic signals in integral membrane proteins. Eur. J. Biochem. **174:**671–678. http://dx.doi.org/10.1111/j.1432-1033.1988.tb14150.x.
37. **Arts J, van Boxtel R, Filloux A, Tommassen J, Koster M.** 2007. Export of the pseudopilin XcpT of the *Pseudomonas aeruginosa* type II secretion system via the signal recognition particle-Sec pathway. J. Bacteriol. **189:**2069–2076. http://dx.doi.org/10.1128/JB.01236-06.
38. **Katz C, Ron EZ.** 2008. Dual role of FtsH in regulating lipopolysaccharide biosynthesis in *Escherichia coli*. J. Bacteriol. **190:**7117–7122. http://dx.doi.org/10.1128/JB.00871-08.
39. **Langklotz S, Schakermann M, Narberhaus F.** 2011. Control of lipopolysaccharide biosynthesis by FtsH-mediated proteolysis of LpxC is conserved in enterobacteria but not in all gram-negative bacteria. J. Bacteriol. **193:**1090–1097. http://dx.doi.org/10.1128/JB.01043-10.
40. **Führer F, Müller A, Baumann H, Langklotz S, Kutscher B, Narberhaus F.** 2007. Sequence and length recognition of the C-terminal turnover element of LpxC, a soluble substrate of the membrane-bound FtsH protease. J. Mol. Biol. **372:**485–496. http://dx.doi.org/10.1016/j.jmb.2007.06.083.
41. **Nichols RJ, Sen S, Choo YJ, Beltrao P, Zietek M, Chaba R, Lee S, Kazmierczak KM, Lee KJ, Wong A, Shales M, Lovett S, Winkler ME, Krogan NJ, Typas A, Gross CA.** 2011. Phenotypic landscape of a bacterial cell. Cell **144:**143–156. http://dx.doi.org/10.1016/j.cell.2010.11.052.
42. **Misra R, Miao Y.** 1995. Molecular analysis of *asmA*, a locus identified as the suppressor of OmpF assembly mutants of *Escherichia coli* K-12. Mol. Microbiol. **16:**779–788. http://dx.doi.org/10.1111/j.1365-2958.1995.tb02439.x.
43. **Deng M, Misra R.** 1996. Examination of AsmA and its effect on the assembly of *Escherichia coli* outer membrane proteins. Mol. Microbiol. **21:**605–612. http://dx.doi.org/10.1111/j.1365-2958.1996.tb02568.x.
44. **Niba ETE, Naka Y, Nagase M, Mori H, Kitakawa M.** 2007. A genome-wide approach to identify the genes involved in biofilm formation in *E. coli*. DNA Res. **14:**237–246. http://dx.doi.org/10.1093/dnares/dsm024.
45. **Ried G, Hindennach I, Henning U.** 1990. Role of lipopolysaccharide in assembly of *Escherichia coli* outer membrane proteins OmpA, OmpC, and OmpF. J. Bacteriol. **172:**6048–6053.
46. **Mahalakshmi S, Sunayana MR, SaiSree L, Reddy M.** 6 November 2013, posting date. *yciM* is an essential gene required for regulation of lipopolysaccharide synthesis in *Escherichia coli*. Mol. Microbiol. [Epub ahead of print.] http://dx.doi.org/10.1111/mmi.12452.
47. **Hanahan D.** 1983. Studies on transformation of *Escherichia coli* with plasmids. J. Mol. Biol. **166:**557–580. http://dx.doi.org/10.1016/S0022-2836(83)80284-8.
48. **Bos MP, Tommassen J.** 2005. Viability of a capsule- and lipopolysaccharide-deficient mutant of *Neisseria meningitidis*. Infect. Immun. **73:**6194–6197. http://dx.doi.org/10.1128/IAI.73.9.6194-6197.2005.
49. **Melchers K, Schuhmacher A, Buhmann A, Weitzenegger T, Belin D, Grau S, Ehrmann M.** 1999. Membrane topology of CadA homologous P-type ATPase of *Helicobacter pylori* as determined by expression of *phoA* fusions in *Escherichia coli* and the positive inside rule. Res. Microbiol. **150:**507–520. http://dx.doi.org/10.1016/S0923-2508(99)00106-0.
50. **Fürste JP, Pansegrau W, Frank R, Blöcker H, Scholz P, Bagdasarian M, Lanka E.** 1986. Molecular cloning of the plasmid RP4 primase region in a multi-host-range *tacP* expression vector. Gene **48:**119–131. http://dx.doi.org/10.1016/0378-1119(86)90358-6.
51. **Vieira J, Messing J.** 1982. The pUC plasmids, an M13mp7-derived system for insertion mutagenesis and sequencing with synthetic universal primers. Gene **19:**259–268. http://dx.doi.org/10.1016/0378-1119(82)90015-4.